Available online at www.sciencedirect.com
ScienceDirect
Catalysis Today 124 (2007) 232–239
CATALYSIS TODAY
www.elsevier.com/locate/cattod

Sonophotocatalytic/H_2O_2 degradation of phenolic compounds in agro-industrial effluents

Adrián M.T. Silva [a,*], Ekaterini Nouli [b], Ângela C. Carmo-Apolinário [a], Nikolaos P. Xekoukoulotakis [b], Dionissios Mantzavinos [b]

[a] *Department of Chemical Engineering, Faculty of Sciences and Technology, University of Coimbra, Polo II—Pinhal de Marrocos, 3030-290 Coimbra, Portugal*

[b] *Department of Environmental Engineering, Technical University of Crete, Polytechneioupolis, GR-73100 Chania, Greece*

Available online 18 May 2007

Abstract

The treatment of a model solution containing 13 compounds typically found in olive mill wastewaters (OMW), at a concentration of 50 mg/L each, by means of sonophotocatalysis over 0.75 g/L Degussa TiO_2 suspensions was studied. Experiments were conducted at an ultrasound frequency and intensity of 80 kHz and 120 W, respectively, ultraviolet power of 9, 250 and 400 W with or without the addition of 0.118 mol/L H_2O_2. Treatment efficiency was assessed following changes in total phenols (TPh) concentration, individual species concentration, chemical oxygen demand (COD), total organic carbon (TOC) and ecotoxicity. In general, photocatalytic degradation increased with increasing UVA power, while sonolysis alone failed to cause any degradation. Process coupling and addition of extra oxidant resulted in substantial levels of degradation. For instance, sonophotocatalytic treatment at 400 W UVA power with H_2O_2 for 120 min resulted in complete mineralization followed by significant toxicity reduction. TiO_2 characterization before and after use showed that the catalyst suffered no composition or morphology changes during treatment. However, a substantial surface area increase was noted and this was attributed to the ultrasound de-aggregating catalyst particles. Preliminary tests with an actual OMW showed that the sonophotocatalytic/H_2O_2 treatment is a promising technology for this type of effluents.

Keywords: Agro-effluents; Catalyst characterization; Phenols; Sonophotocatalysis; TiO_2

1. Introduction

Olive mill waste waters (OMW) constitute a major environmental problem in the Mediterranean region. The classical discontinuous olive oil process has been progressively replaced by continuous centrifugation using three-phase systems and, more recently, two-phase systems because the latter consume lower quantities of water and generate 50% less OMW per unit mass of olive. Nonetheless, in countries like Portugal and Greece most of the mills still operate with the classical and the three-phase olive extraction processes. Discharge of these effluents to water bodies damages seriously the self-capabilities of these environments. Moreover, spreading of OMW onto the fields can reach and contaminate the waterbed due to the associated biorecalcitrant characteristics [1]. Biological treatments are highly affected by the large amounts of phenolic compounds typically found in this kind of effluents and, therefore, other technologies may be needed for the partial or complete treatment of OMW.

Photocatalysis is an active area of research in environmental protection, while the development and application of ultrasound-based processes begin to play an important role in this domain. The first treatment is based on the photonic activation of the catalyst by light irradiation and the second on the ultrasonically induced acoustic cavitation [2]. Both processes predominantly involve the formation of free radicals and other reactive moieties which consequently react with and destroy the pollutant species. The mechanisms via which these processes mainly occur have been comprehensively presented in the literature [2,3]. Concerning photocatalysis with titanium dioxide as the catalyst, electrons in conduction band (e_{cb}^-) and holes in the valence band

* Corresponding author. Present address: Laboratory of Catalysis and Materials, Chemical Engineering Department, Faculty of Engineering – University of Porto (FEUP), Rua Dr. Roberto Frias, 4200-465 Porto – Portugal. Tel.: +351 964291576/225081998; fax: +351 225081449.
E-mail addresses: adrian@fe.up.pt, adrian@eq.uc.pt (A.M.T. Silva), mantzavi@mred.tuc.gr (D. Mantzavinos).

0920-5861/$ – see front matter
doi:10.1016/j.cattod.2007.03.057

(h_{vb}^+) are produced when the catalyst is irradiated with light energy higher than its band gap energy E_{bg} ($h\nu \geq E_{bg}$), according to reactions (1)–(8) [2,4]:

$$TiO_2 + h\nu\,(UV\,\lambda < 400\,nm) \rightarrow TiO_2(e_{cb}^- + h_{vb}^+) \quad (1)$$

$$h_{vb}^+ + H_2O \rightarrow H^+ + HO^\bullet \quad (2)$$

$$h_{vb}^+ + HO^- \rightarrow HO^\bullet \quad (3)$$

$$\text{Organic molecule} + h_{vb}^+ \rightarrow \text{oxidation products} \quad (4)$$

$$e_{cb}^- + O_2 \rightarrow O_2^{\bullet -} \quad (5)$$

$$O_2^{\bullet -} + H^+ \rightarrow HO_2^\bullet \quad (6)$$

$$\text{Organic molecule} + e_{cb}^- \rightarrow \text{reduction products} \quad (7)$$

$$\text{Radicals}\,(HO^\bullet, HO_2^\bullet) + \text{organic compounds} \rightarrow \text{degradation products} \quad (8)$$

Regarding sonochemical processes, ultrasound irradiation of aqueous solutions in the range 20–1000 kHz induces acoustic cavitation, which can be defined as the cyclic formation, growth and subsequent collapse of micro-bubbles or cavities occurring in extremely small intervals of time and releasing large quantities of energy over a small location. Thus, cavitation serves as a mean of concentrating the diffuse energy of ultrasound into hot spots that behave as micro-reactors. In aqueous phase sonolysis, there are three potential sites for sonochemical activity, namely: (i) the gaseous region of the cavitation bubble where volatile and hydrophobic species are easily degraded through pyrolytic reactions as well as reactions involving the participation of hydroxyl radicals with the latter being formed through water sonolysis, (ii) the bubble-liquid interface where hydroxyl radicals are localized and, therefore, radical reactions predominate although pyrolytic reactions may also, to a lesser extent, occur and (iii) the liquid bulk where secondary sonochemical activity may take place mainly due to free radicals that have escaped from the interface and migrated to the liquid bulk.

Although photocatalysis and sonolysis have been extensively employed individually for the degradation of several organic species in water, their combined use (i.e. sonophotocatalysis) has received appreciably less attention. Process integration may be favorable in eliminating the disadvantages associated with each individual process, thus increasing degradation rates. For instance, in heterogeneous catalytic systems, the use of ultrasound creates conditions of increased turbulence in the liquid, thus decreasing mass transfer limitations and increasing the surface area available due to catalyst fragmentation and de-agglomeration [5]. Sonophotocatalysis has been studied for the degradation of model compounds such as salicylic acid [6], propyzamide [7], 1,4-dioxane [8], 2-(butylamino)ethanethiol [9], 2-chlorophenol [10,11], dyes [12] and MTBE [12,13]. Unlike the number of publications dealing with the sonophotocatalytic degradation of single model solutions, fewer studies have dealt with complex synthetic and/or actual effluents.

In this respect, the aim of this work was to study the efficiency of photocatalysis alone, sonolysis alone and their combination (sonophotocatalysis) in the presence and absence of H_2O_2 for the treatment of (i) a complex synthetic solution containing 13 compounds typically found in OMW, and (ii) an actual OMW. To the best of our knowledge this is the first report dealing with the sonophotocatalysis of the main aromatic compounds found in agro-industrial effluents.

2. Experimental

2.1. Materials

Cinnamic ($C_9H_8O_2$ ≥99%), *p*-coumaric (*p*-hydroxycinnamic, $C_9H_8O_3$ ≥98%), *o*-coumaric (*o*-hydroxycinnamic, $C_9H_8O_3$ ≥97%), caffeic (3,4-dihydroxycinnamic, $C_9H_8O_4$ ≈97%), ferulic (4-hydroxy-3-methoxycinnamic, $C_{10}H_{10}O_4$ ≥98%), syringic (3,5-dimethoxy-4-hydroxybenzoic, $C_9H_{10}O_5$ ≥97%), vanillic (4-hydroxy-3-methoxybenzoic, $C_8H_8O_4$ ≥97%), gallic (3,4,5-trihydroxybenzoic, $C_7H_6O_5{\cdot}H_2O$ ≥98%) and 4-hydroxybenzoic ($C_7H_6O_3$ ≈99%) acids as well as resorcinol (*m*-dihydroxybenzene, $C_6H_6O_2$ ≥99%) were obtained from Fluka. Pyrocatechol (1,2-dihydroxybenzene, $C_6H_6O_2$ ≥99%), veratric (3,4-dimethoxybenzoic, $C_9H_{10}O_4$ ≥98%) and protocatechuic (3,4-dihydroxybenzoic, $C_7H_6O_4$ ≥98%) acids were supplied by Sigma. These 13 compounds typically found in OMW were used to prepare a model solution at a concentration of 50 mg/L each, yielding COD_0 = 1141 mg/L, TOC_0 = 433 mg/L and TPh_0 = 650 mg/L. Other properties are shown in Table 1.

The actual OMW was collected during the harvest season (November 2005) from a three-phase continuous olive mill plant located at Chania, Western Crete, Greece. The raw effluent was first filtered to remove the solid content and then diluted 10 times with deionized water to yield an effluent with COD_0 = 8040 mg/L, TOC_0 = 1932 mg/L and TPh_0 = 729 mg/L. Other properties are shown in Table 1.

Folin–Ciocalteu's phenol reagent and sodium carbonate were purchased from Sigma–Aldrich and used for total phenols determination. Methanol (≥99.9%) and acetonitrile (99.8%) used in high performance liquid chromatography were supplied by Merck. Hydrogen peroxide 35% (w/w) was obtained from Fluka. Ultrapure water was produced in an EasyPureRF system (Barnstead/Thermolyne, USA).

The TiO_2 catalyst used in this work was Aeroxide P25 supplied by Degussa AG consisting of 80% anatase and 20%

Table 1
Properties of model solution and actual OMW before and after H_2O_2-assisted sonophotocatalysis at 400 W (nd: not determined)

Properties	Model solution			Olive mill wastewater		
	0 min	120 min	Reduction (%)	0 min	120 min	Reduction (%)
COD (mg/L)	1141	16	99	8040	nd	nd
TOC (mg/L)	433	7	98	1932	1129	42
TPh (mg/L)	650	0	100	729	194	73
pH	3.5	5.5	–	4.8	4.0	–
Toxicity (%)	100	37	63	100	100	0

rutile; previous studies have shown that this low cost and relatively stable material is a very effective catalyst for the sonophotocatalytic degradation of various organic compounds [6,9,10,12].

2.2. Sonophotoreactor and experimental procedures

Batch experiments were performed in a borosilicate glass reactor (Ace Glass Vineland, NJ, USA). The reactor consists of an external cylindrical reaction vessel (310 $mm_L \times 73\ mm_{i.d.}$) containing 0.35 L of the model or actual wastewater, and an internal double-walled compartment (390 $mm_L \times 53\ mm_{i.d.}$) inside which the UV lamp is housed. In all the experiments (with and without ultrasound) temperature was maintained constant at $31 \pm 1\ ^\circ C$ through the use of cooling water circulating through the double-walled compartment, thus acting as cooling water jacket, while air was continuously sparged in the liquid. UVA irradiation was provided by a 9 W UVA lamp (Radium Ralutec, 9 W/78, 350–400 nm) as well as 250 and 400 W medium pressure mercury vapor lamps (Osram HQL MBF-U) both of which emit predominantly at 366 nm. A titanium horn immersed in the solution and connected to an Ultrason 250 (LabPlant, UK) ultrasound generator operating at 80 kHz frequency and a power output of 120 W was used for sonication experiments.

Different treatments were tested, namely: TiO_2 photocatalysis (UV), sonolysis (US), combined photocatalysis and sonolysis (US + UV), H_2O_2-assisted photocatalysis (UV + H_2O_2) and H_2O_2-assisted combined photocatalysis and sonolysis (US + UV + H_2O_2). For photocatalytic and sonophotocatalytic experiments a TiO_2 concentration of 0.75 g/L was used, while in those cases where H_2O_2 was used as an extra oxidant, its concentration was 0.118 mol/L. These values were chosen since preliminary experiments had shown that treatment efficiency remained practically unchanged at catalyst and oxidant concentrations greater than these values. The catalyst was slurried in the reaction mixture and magnetically stirred for 30 min in the dark to ensure total equilibrium of adsorption/desorption of chemical compounds on the catalyst surface. Following this period of time, the lamp and/or the ultrasound generator were turned on with the simultaneous addition (if needed) of H_2O_2 and this was taken as the starting point ($t = 0$) of the reaction. Samples were periodically withdrawn from the reaction vessel and filtered through 0.45 μm disposable filters (*Minisart RC25*, Sartorious) in order to separate the TiO_2 particles prior to analysis.

2.3. Analytical techniques

2.3.1. Total phenol content (TPh)

Samples were analyzed with respect to their phenolic content (TPh) using the Folin–Ciocalteu reagent [14]. Twenty microliters of sample were introduced in a 2 mL cuvette and 100 μL of the Folin–Ciocalteu reagent were added as well as 1.58 mL of water. After 3–6 min 300 μL of a saturated sodium carbonate solution were added and the resulting solution was left in the dark for 2 h. Absorbance was determined with a UNICAM Heλios spectrometer at 750 nm against a blank solution containing 20 μL of water instead of 20 μL of sample. The calibration curve ($r = 0.9997$) was prepared using gallic acid and, therefore, TPh values are reported as gallic acid equivalent.

2.3.2. High performance liquid chromatography (HPLC)

The concentration of each compound in the model solution was followed by means of a computer controlled Shimadzu HPLC system equipped with diode array (SDP-$M10A_{Vp}$) and fluorescence (RF-$10A_{XL}$) detectors and an Alltech Inertsil C8 5 μm, 250 mm × 4.6 mm column. An optimized gradient elution was used with detection at 260 nm and a flowrate of 1 mL/min. Firstly, the column was equilibrated with an A:B (10:90) mixture of 1% acetic acid and 0.5% acetonitrile in methanol (A) and 1% acetic acid in water (B), with isocratic elution during 15 min followed by a linear gradient run to A:B (60:40) in 27 min and finally to A:B (10:90) in 5 min.

This method proved useful for the successful separation and subsequent quantification of all compounds but ferulic and veratric acids and pyrocatechol. The latter could not be detected at the chromatographic conditions in question due to weak detection response. Ferulic and veratric acids eluted together from the column and, therefore, they were quantified as a single compound; this could be done without significant error since both compounds had similar detection responses.

2.3.3. Chemical oxygen demand (COD) and total organic carbon (TOC)

For COD measurements, commercially available digestion solutions (Hach) incubated for 2 h at 150 °C in a COD reactor (Model 45600, Hach) were used; COD was determined colorimetrically in a Hach DR/2010 spectrophotometer. TOC was determined with a Shimadzu 5000 TOC analyzer, whose operation is based on the combustion/non-dispersive infrared gas analysis method (NDIR).

2.3.4. Toxicity

Toxicity was evaluated according to ASTM standards (Standard Guide E1440-91) using the Rotoxkit M for the development of estuarine/marine toxicity screening tests. The test employs juveniles of rotifer *Brachionus plicatilis*, obtained from uniform cysts after three parthenogenetic generations. In brief, the cysts to hatch are placed on a ''multiwell'' plate at a reduced salinity, 25 °C and constant lighting for 28–30 h before the test starts. The assay is done within 2 h after the eclosion of the cysts. For that purpose five organisms are placed in each of the 36 wells of the plate, which have previously been fulfilled with the aqueous sample to be tested (control + five samples with six replicates). After 24 h the death organisms are counted, and LC_{50} is determined.

2.3.5. BET surface area, X-ray diffraction (XRD) and scanning electron microscopy (SEM)

Brunauer–Emmett–Teller (BET) surface area and the average pore diameter were measured with an ASAP 2000 instrument from Micromeritics using nitrogen (−196 °C). XRD

analysis was carried out at ambient temperature with a Philips PW 3040/00 XPert X-ray analyzer (Co Kα radiation, λ = 1.78897 Å) with 40 kV, 35 mA, data recorded at a 0.04° step size for 1 s at each step. SEM analysis at different scales/magnifications was performed in a JEOL JSM-5310 scanning microscope. The powder samples were deposited on adhesive tape and fixed on a support coated with gold.

3. Results and discussion

3.1. Degradation of total phenols in model solution by sonolysis, photocatalysis and sonophotocatalysis

Fig. 1a–c shows TPh concentration–time profiles during the photocatalytic, sonolytic and sonophotocatalytic treatment of model solution as a function of UVA irradiation intensity and the addition of hydrogen peroxide. Fig. 1a clearly shows that photocatalytic treatment alone at 9 W had practically no effect on TPh degradation after 180 min of reaction; nonetheless, increasing UVA intensity at 400 W was capable of achieving 46% TPh degradation. Sonolysis alone at 80 kHz, 120 W led to no conversion after 180 min of reaction. However, coupling sonolysis with photocatalysis led to considerably increased degradation rates. For instance, coupling photocatalysis at 400 W with sonolysis led to 95% conversion after 150 min of reaction, while the respective value with photocatalysis alone was only 36%.

Addition of hydrogen peroxide enhanced markedly the rate of sonophotocatalytic degradation (Fig. 1b); for instance, complete TPh conversion was achieved after about 45 min at 400 W with H_2O_2, while the respective value without H_2O_2 was about 37%. This effect was less pronounced for the runs at 9 W. In fact, hydrogen peroxide enhances photocatalysis either with or without sonolysis, as can be seen by comparison of Fig. 1c with a. Moreover, the improvement achieved by sonolysis in the combined system (Fig. 1c) is generally less characteristic than the effect of hydrogen peroxide in the sonophotocatalytic reactions (Fig. 1b).

Therefore, the results of Fig. 1a–c clearly shows that, at the conditions in question, (i) the efficiency of photocatalytic degradation is a strong function of the applied UVA irradiation intensity, (ii) sonochemical reactions act synergistically to ultraviolet irradiation, thus leading to substantially increased reaction rates, and (iii) addition of hydrogen peroxide promotes photocatalytic and sonophotocatalytic reactions.

The beneficial effect of coupling photocatalysis with sonolysis as well as adding hydrogen peroxide can be attributed to the increased production of hydroxyl radicals in the reaction system through the following steps, reactions (9)–(14) [2,4,15]: (i) water sonolysis (reactions (9) and (10)), (ii) reaction of hydrogen peroxide with the hydrogen atoms formed from water sonolysis (reaction (11)), (iii) hydrogen peroxide photolytic dissociation (reaction (12)), (iv) reaction of hydrogen peroxide with the superoxide radical anions formed during photocatalysis (reaction (13)), (v) reaction of hydrogen peroxide with conduction band

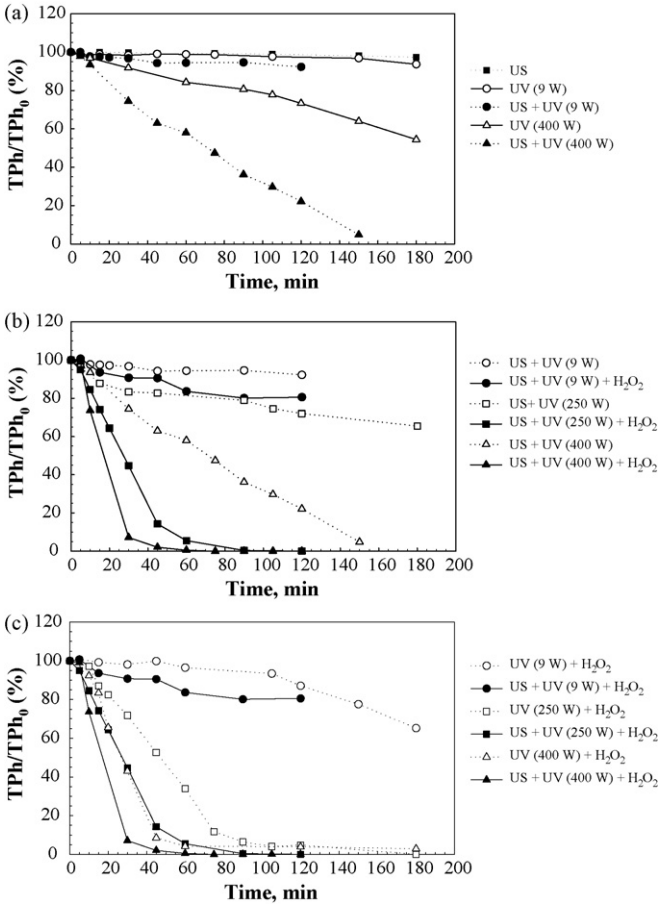

Fig. 1. Normalized total phenol concentration–time profiles of model solution during: (a) sonolysis, photocatalysis and sonophotocatalysis at various UVA intensities in the absence of hydrogen peroxide; (b) sonophotocatalysis at various UVA intensities in the presence of hydrogen peroxide; (c) photocatalysis with and without sonolysis at various UVA intensities in the presence of hydrogen peroxide.

electrons (reaction (14)):

$$H_2O + \text{ultrasound} \rightarrow H^\bullet + HO^\bullet \quad (9)$$

$$H_2O + \text{ultrasound} \rightarrow \tfrac{1}{2}H_2 + \tfrac{1}{2}H_2O_2 \quad (10)$$

$$H_2O_2 + H^\bullet \rightarrow H_2O + HO^\bullet \quad (11)$$

$$H_2O_2 + h\nu \rightarrow 2HO^\bullet \quad (12)$$

$$H_2O_2 + O_2^{\bullet -} \rightarrow HO^\bullet + HO^- + O_2 \quad (13)$$

$$H_2O_2 + e_{cb}^- \rightarrow HO^\bullet + HO^- \quad (14)$$

An attempt was made to derive the kinetics of TPh sonophotocatalytic degradation. Previous studies [16] have shown that the kinetics of TPh photocatalytic degradation can be described by a zero-order kinetic expression concerning phenols concentration, i.e. Eq. (15):

$$r_{TPh} = -\frac{dTPh}{dt} = k_{obs} \Leftrightarrow TPh_0 - Tph = k_{obs}t \quad (15)$$

where k_{obs} is the reaction rate constant and t is the reaction time. Fig. 2a shows the results of Fig. 1b plotted in the form of

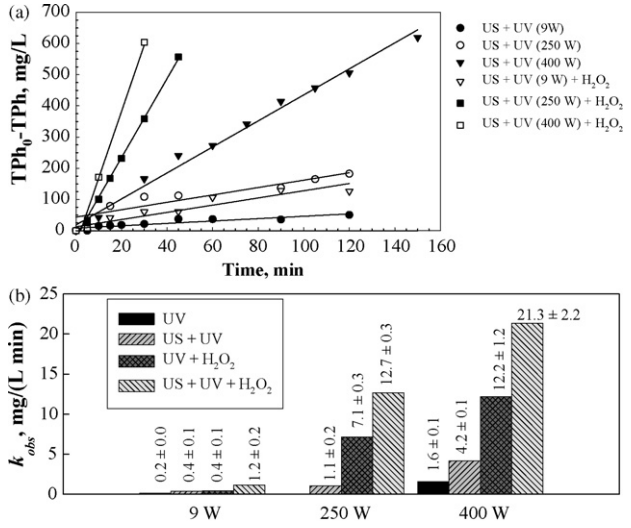

Fig. 2. Zero-order kinetics with respect to phenol concentration for various treatment schemes. (a) Plot of Eq. (15) for the data of Fig. 3; (b) comparison of k_{obs} values for various treatments.

Eq. (15) showing that, indeed, the reaction appears to be zero-order on TPh concentration. From the resulting straight lines, one can compute rate constant values and these are shown in Fig. 2b; values from photocatalytic experiments are also given alongside sonophotocatalytic reactions. The synergy between photocatalysis and sonolysis is demonstrated for the experiment at 400 W UVA irradiation; the rate constant for sonophotocatalysis ($k_{US + UV}$) is 4.2 ± 0.1 and this is higher than the sum of the individual rate constants for photocatalysis (k_{UV} = 1.6 ± 0.1) and sonolysis (k_{US} = 0).

3.2. Degradation of individual phenolic compounds by H_2O_2-assisted sonophotocatalysis

Changes in the concentration of individual compounds in the model solution were followed by means of HPLC during the H_2O_2-assisted sonophotocatalytic treatment and representative results from the run performed at 250 W UVA intensity are shown in Fig. 3. Fig. 3a shows concentration–time profiles of benzoic acid derivatives, while Fig. 3b shows profiles of cinnamic acid derivatives as well as resorcinol. As already mentioned before, ferulic and veratric acids could not be separated at the chromatographic conditions in question as they had a common retention time and, consequently, they were quantified together as a single moiety; their profile is shown in Fig. 3c. As clearly seen, complete destruction of all compounds could be achieved within 60 min of reaction. For cinnamic acid derivatives, the reactivity within the early stages of the reaction (e.g. the first 20 min) follows the order (number of hydroxyl groups in brackets): cinnamic (0 OH) > *p*-coumaric (1 OH) > *o*-coumaric (1 OH) > caffeic (2 OH). For benzoic acid derivatives, the order is (number of hydroxyl and methoxy groups in brackets): syringic (1 OH–2 OMe) > 4-hydroxybenzoic (1 OH) ≈ gallic (3 OH) > vanillic (1 OH–1 OMe) > protocatechuic (2 OH). Reactivity appears to depend on the number and type of functional groups attached to the molecule and generally increases with decreasing number of OH groups. Moreover, for the same number of total functional groups, compounds with more methoxy groups seem to be more readily susceptible to degradation than those with more hydroxyl groups (e.g. comparison between syringic and gallic acids or vanillic and protocatechuic acids).

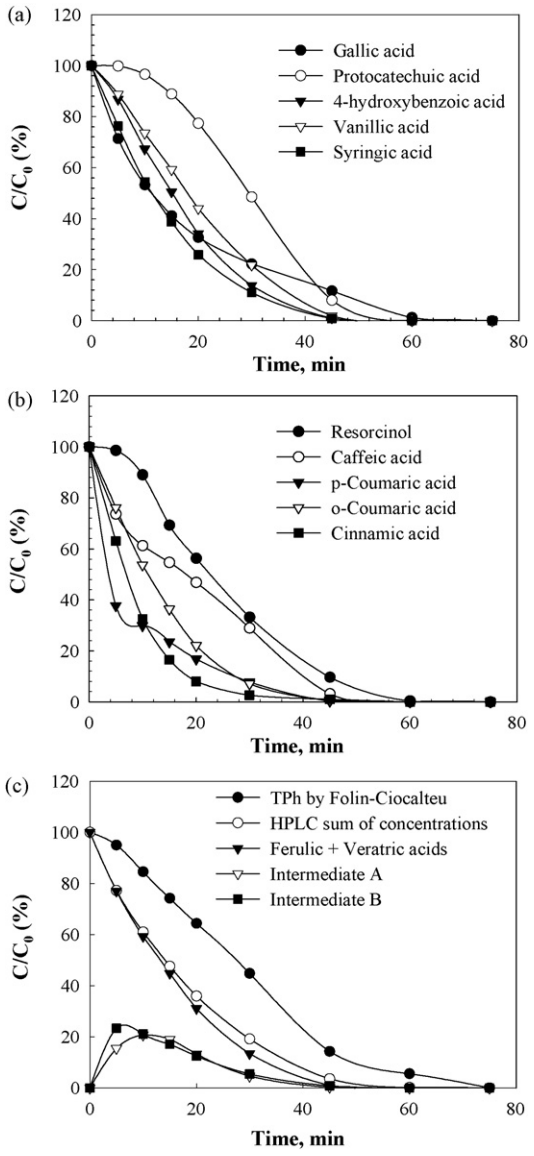

Fig. 3. Normalized concentration–time profiles of (a) of benzoic acid derivatives; (b) cinnamic acid derivatives and resorcinol; (c) ferulic and veratric acids, total phenols and unidentified intermediates during H_2O_2-assisted sonophotocatalysis of model solution at 250 W.

Fig. 3c also shows a comparison between the total phenol concentration as determined by the Folin–Ciocalteu protocol and that calculated from the sum of the individual concentrations obtained by means of HPLC analysis. Since TPh concentration is always greater than the sum of individual concentrations (the discrepancy between the two values is up to about 30%), it can safely be assumed that the degradation of phenolic compounds originally present in the reaction mixture is accompanied by the formation of several phenolic (and indeed other) intermediate compounds. In fact, two major

unknown intermediates were detected during the reaction, referred to as A and B in Fig. 3c (in this case, changes in normalized concentration (C/C_0) were calculated taking the initial concentration of the ferulic + veratric acids mixture as a reference value). These intermediates were formed during the first 10 min of the reaction and rapidly degraded thereafter.

3.3. Degradation of OMW by H_2O_2-assisted sonophotocatalysis

In further experiments, the H_2O_2-promoted sonophotocatalytic process at 400 W was employed to treat actual OMW. A preliminary run was performed where the effluent was subjected to sonolysis alone resulting in only about 7% TPh reduction after 60 min; however, coupling sonolysis with photocatalysis in the presence of H_2O_2 increased degradation to 38%. Fig. 4a shows the extent of TPh conversion as a function of treatment time, while Fig. 4b shows super-imposed chromatograms of OMW samples taken before and after treatment at various times. As seen, 73% TPh reduction was achieved after 120 min, while most of the peaks originally present in the effluent disappeared upon prolonged oxidation. This was accompanied by a 42% TOC reduction after 120 min (Table 1), implying that phenols degradation by-products as well as other compounds originally present in the effluent were relatively resistant to further total oxidation. The original effluent was highly ecotoxic and toxicity remained unchanged after treatment. Fig. 4a and Table 1 also show representative results from the respective run with the model solution. Nearly complete TPh reduction could be achieved within 30 min, while complete mineralization occurred after 120 min. The model solution was highly toxic before treatment but toxicity decreased by 63% upon mineralization. It is believed that the remaining toxicity is due to the unreacted H_2O_2, which has strong disinfection properties and is toxic to microorganisms [17]. From Fig. 4a and Table 1, it is clear that TPh degradation for the model solution is much faster than that for the actual OMW although both effluents have a comparable initial phenolic content. This is presumably due to the fact that the actual effluent also contains several other organics that compete with phenolics for radicals and other reactive moieties and this is consistent with the fact that the OMW COD content is as much as about seven times that of the model solution. Moreover, the actual effluent may also contain radical scavengers, such as carbonate and bicarbonate ions and this would also explain reduced degradation rates. The dark color of OMW may also be responsible for decreased conversions since light penetration may, to some extent, be hindered.

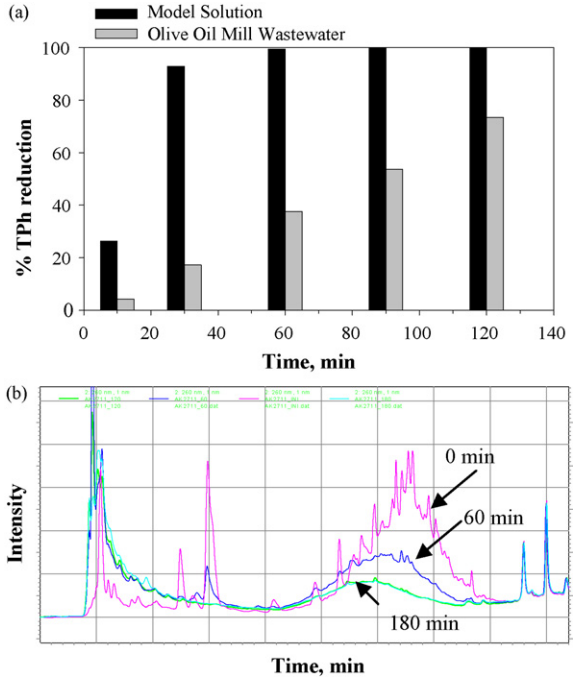

Fig. 4. H_2O_2-assisted sonophotocatalysis of OMW at 400 W. (a) Extent of TPh reduction; (b) super-imposed HPLC chromatograms taken before and after treatment.

3.4. Catalyst characterization

Nitrogen adsorption isotherms of fresh (Fig. 5a) and used (Fig. 5b) TiO_2 show a type II isotherm with a hysteresis loop

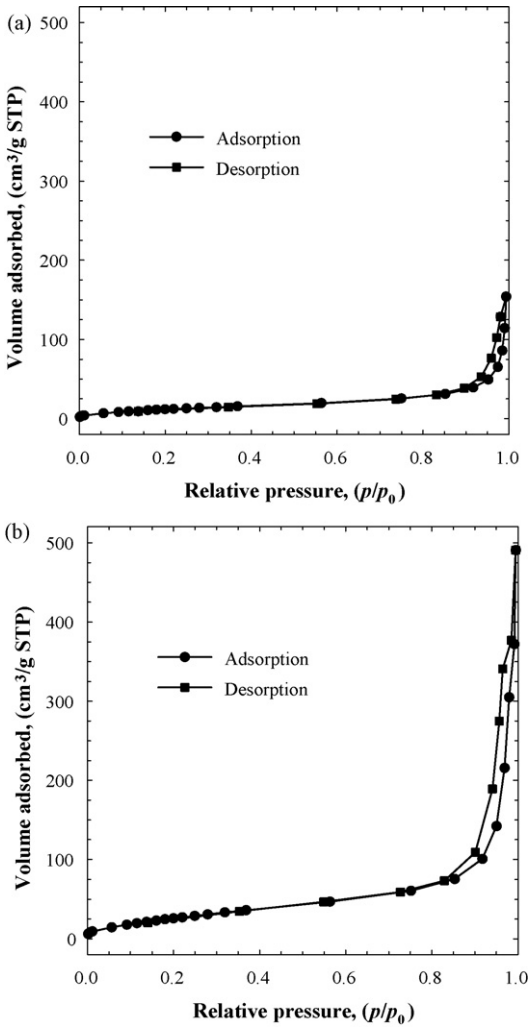

Fig. 5. Adsorption/desorption isotherms of TiO_2 (a) before and (b) after H_2O_2-assisted sonophotocatalysis of model solution at 400 W.

in the high range of relative pressure and suggest an intermediate behavior between hysteresis type H1 and H3 (according to IUPAC classification [18]). The observed isotherm does not exhibit any limiting adsorption at high relative pressures, which is typical of type H3; however, almost vertical and nearly parallel branches are observed over an appreciable range of gas uptake, characteristic of type H1. The hysteresis loop type H1 is characteristic of agglomerates (particles rigidly joined together) or compacts of approximately uniform spheres in fairly regular array, meanwhile, the type H3 is observed with aggregates of plate-like particles giving rise to slit-shape pores.

Although the fresh and used catalyst samples both gave the same type of isotherm, the latter was capable of adsorbing far greater nitrogen volumes than the former. In fact, the fresh TiO_2 catalyst had a BET surface area of 47.3 m^2/g and after 180 min of H_2O_2-assisted sonophotocatalytic treatment this value increased to 109.7 m^2/g (Table 2). This marked increase in BET surface area may be attributed to the ultrasound de-aggregating catalyst particles, which in turn would increase both surface area and catalyst activity. Therefore, the synergistic contribution of sonolysis to photocatalysis may be twofold offering: (i) increased production of hydroxyl radicals according to reactions (9) and (11), and (ii) increased catalyst surface area. Moreover, one can also observe that the average pore diameter of the fresh and used catalyst samples was 20.1 and 27.7 nm, respectively. These values are in the range of mesoporous structures, namely 2–50 nm [18].

XRD patterns as well as SEM photographs of the fresh and used catalyst samples are shown in Fig. 6. The peak at $2\theta = 29.5^\circ$ is the major characteristic peak denoting an anatase structure followed by peaks at $56.4^\circ > 63.6^\circ \approx 44.3^\circ > 65^\circ > 74.4^\circ > 90.2^\circ$. On the other hand, peaks related to rutile were also found, namely at $32.1^\circ > 42.2^\circ > 48.4^\circ > 67^\circ > 76.2^\circ > 51.7^\circ$. XRD patterns and SEM photographs of the fresh catalyst sample were quite similar to those of the used one, pointing out that the crystalline catalyst structure was not affected during the sonophotocatalytic treatment. The catalyst seems to consist of aggregates/agglomerates of spherical and irregular particles with diameters below 1 μm.

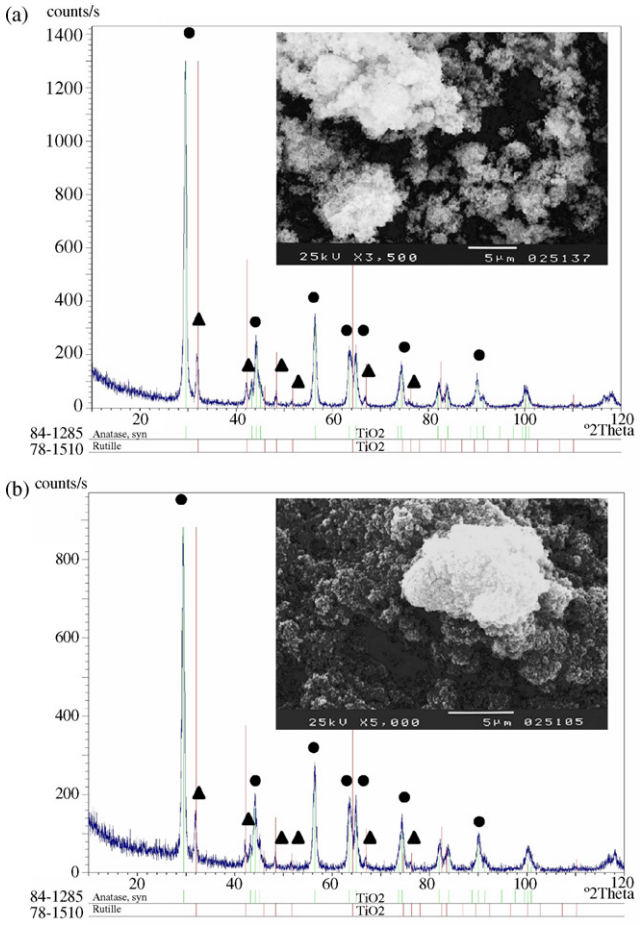

Fig. 6. XRD patterns and SEM images (inset) of TiO_2 (a) before and (b) after H_2O_2-assisted sonophotocatalysis of model solution at 400 W. (●) Anatase; (▲) rutile.

3.5. Cost evaluation

Advanced oxidation processes based on artificial light and/or ultrasound irradiation may be associated with increased operating costs, a major fraction of which is related to electric energy consumption. Bolton et al. [19] introduced the concept of electric energy consumption per unit mass of pollutant destroyed (E_{EM}) assuming that the removal rate is directly proportional to the rate of electric energy use, i.e. Eq. (16) for zero-order reactions:

$$E_{EM} = \frac{Pt \times 10^6}{V(C_0 - C)} \quad (16)$$

where V is the effluent volume, t the respective treatment time and P is the applied power. Based on the time needed to achieve at least 90% TPh removal, energy consumption as well as treatment costs were calculated for various combinations and representative results are shown in Table 3. In general, increased UVA irradiation intensities and/or addition of H_2O_2 effectively reduce the treatment time required to achieve 90% TPh removal. In this respect, increased treatment costs associated with increased energy consumption and/or the use of costly H_2O_2 can be compensated by the reduced treatment times needed.

Table 2
BET surface area and pore diameter of TiO_2 samples before and after H_2O_2-assisted sonophotocatalysis at 400 W

Sample	BET surface area (m^2/g)	Average pore diameter (nm)
Fresh	47.3 ± 0.7	20.1
Used	109.7 ± 1.6	27.7
Increase (%)	132	38

Table 3
Cost evaluation for different treatments in terms of energy and H_2O_2 consumption for ≥90% TPh removal

Type of effluent	Type of treatment	Time (min)	Electric energy consumption			Energy cost €/L[a]	Total cost €/L[b]
			kWh	kWh/kg	kWh/L		
Model	UV(250 W) + H_2O_2	90	0.38	1761	1.07	0.05	0.06
Model	UV(400 W) + H_2O_2	45	0.30	1441	0.86	0.04	0.05
Model	US + UV (400 W)	150	1.30	5996	3.71	0.19	0.19
Model	US + UV(250 W) + H_2O_2	60	0.37	1721	1.06	0.05	0.06
Model	US + UV(400 W) + H_2O_2	30	0.26	1230	0.74	0.04	0.05
OMW	US + UV(400 W) + H_2O_2	120	1.04	5559	2.97	0.15	0.16

Basis of calculations: [a]0.05 €/kWh. [b]0.70 €/L of H_2O_2.

4. Conclusions

The conclusions drawn from this study are summarized as follows:

(1) Sonophotocatalytic treatment of a synthetic solution containing several phenolic compounds typically found in agro-industrial effluents over Degussa TiO_2 suspensions proved efficient in terms of specific pollutants removal and solution mineralization. Interestingly, the combined process was considerably more effective than the respective individual treatments, i.e. sonolysis and photocatalysis. Process efficiency was further enhanced in the presence of H_2O_2 acting as hydroxyl radical source.
(2) Composition and morphology of the catalyst were not considerably affected during the sonophotocatalytic treatment. However, the BET surface area of the used catalyst was much higher than that of the fresh one, suggesting possible particle de-aggregation induced by the ultrasound.
(3) The synergistic action of ultrasound may be associated with an increase in the production of hydroxyl radicals via water sonolysis and H_2O_2 cleavage as well as an increase in catalyst surface area. Moreover, the ultrasound may accelerate mass transfer of reagents onto the TiO_2 surface as well as remove any impurities from its surface.
(4) Screening tests with actual OMW gave promising results as the combined process may achieve reasonable levels of organic pollutant destruction.

Acknowledgments

Adrián M.T. Silva gratefully acknowledges the Fundação para a Ciência e Tecnologia, Ministério da Ciência e do Ensino Superior, Portugal, for financial support under the Programa Operacional de Ciência e Inovação 2010. The authors wish to thank Dr M. Ruiz for her involvement with toxicity analysis and Degussa A.G. for providing the catalyst.

References

[1] M. Niaounakis, C.P. Halvadakis, in: C. Stavropoulos (Ed.), Olive-Mill Waste Management, Literature Review and Patent Survey, Typothito-George Dardanos Publications, Athens, Greece, 2004, p. 3.
[2] A. Mills, S.-K. Lee, T.J. Mason, C. Pétrier, in: S. Parsons (Ed.), Semiconductor Photocatalysis in Advanced Oxidation Processes for Water and Wastewater Treatment, IWA Publishing, London, UK, 2004, p. 137.
[3] Y.G. Adewuyi, Environ. Sci. Technol. 39 (2005) 8557.
[4] I.K. Konstantinou, T.A. Albanis, Appl. Catal. B: Environ. 49 (2004) 1.
[5] P.R. Gogate, A.B. Pandit, AIChE J. 50 (2004) 1051.
[6] L. Davydov, E.P. Reddy, P. France, P.G. Smirniotis, Appl. Catal. B: Environ. 32 (2001) 95.
[7] J. Yano, J.-i. Matsuura, H. Ohura, S. Yamasaki, Ultrason. Sonochem. 12 (2005) 197.
[8] A. Nakajima, M. Tanaka, Y. Kameshima, K. Okada, J. Photochem. Photobiol. A: Chem. 167 (2004) 75.
[9] A.V. Vorontsov, Y.-C. Chen, P.G. Smirniotis, J. Hazard. Mater. B113 (2004) 89.
[10] V. Ragaini, E. Selli, C.L. Bianchi, C. Pirola, Ultrason. Sonochem. 8 (2001) 251.
[11] M. Mrowetz, C. Pirola, E. Selli, Ultrason. Sonochem. 10 (2003) 247.
[12] M. Bertelli, E. Selli, Appl. Catal. B: Environ. 52 (2004) 205.
[13] E. Selli, C.L. Bianchi, C. Pirola, M. Bertelli, Ultrason. Sonochem. 12 (2005) 395.
[14] O. Folin, V. Ciocalteu, J. Biolog. Chem. LXXIII (1927) 627.
[15] H. Harada, Ultrason. Sonochem. 8 (2001) 55.
[16] A.M.T. Silva, E. Nouli, N.P. Xekoukoulotakis, D. Mantzavinos, Appl. Catal. B: Environ. 73 (2007) 11.
[17] T. Velegraki, I. Poulios, M. Charalabaki, N. Kalogerakis, P. Samaras, D. Mantzavinos, Appl. Catal. B: Environ. 62 (2005) 159.
[18] K.S.W. Sing, D.H. Everett, R.A.W. Haul, L. Moscou, R.A. Pierotti, J. Rouquérol, T. Siemieniewska, Pure Appl. Chem. 57 (1985) 603.
[19] J.R. Bolton, K.G. Bircher, W. Tumas, C.A. Tolman, Pure Appl. Chem. 73 (2001) 627.